

WETTABILITY OF THE FINE FIBRE SHEET PREPARED FROM OIL PALM EMPTY FRUIT BUNCHES

Kose R¹, Utsumi M², Yatsui H², Tun-Abdul-Aziz MK³ & Okayama T¹, *

¹Division of Natural Resources and Ecomaterials, Institute of Agriculture, Tokyo University of Agriculture and Technology, 3-5-8, Saiwai-cho, Fuchu-shi, Tokyo, 183-8509, Japan

²Department of Environmental and Natural Resource Sciences, Faculty of Agriculture, Tokyo University of Agriculture and Technology, 3-5-8, Saiwai-cho, Fuchu-shi, Tokyo, 183-8509, Japan

³Department of Chemical and Process Engineering, University of Nottingham, Semenyih Selangor, 43500, Malaysia

*okayama@cc.tuat.ac.jp

Submitted July 2017; accepted February 2018

Empty Fruit Bunches (EFB) are byproducts in the palm oil industry. Recently, many studies focused on the application of EFB to pulp fibre and paper. In this study, we used a nanoengineered mechanical treatment, aqueous counter collision (ACC), to investigate the miniaturisation behavior of chemical EFB pulp fibre and compared it with chemical hardwood pulp fibre. Furthermore, a sheet was prepared from fine EFB fibre produced by ACC to examine the wettability. The miniaturisation of the EFB pulp fibre using ACC progressed more quickly than that of hardwood pulp fibre, and finally, nanofibre was obtained from the EFB. The width of nanofibre was the same as hardwood chemical pulp fibre. A drop of water didn't penetrate into the sheet but spread on the sheet surface within 10 s. The water contact angle of the fine EFB fibre sheet depended strongly on the number of collision in ACC treatment than that of the fine hardwood fibre sheet.

Keywords: Agricultural byproduct, aqueous counter collision, EFB fibre, contact angle

INTRODUCTION

Palm oil is one of the most important commercial products in Malaysia, and its production accounted for 20 million tons in 2014 (FAO 2014). Palm oil mills produce a large amount of agricultural byproducts such as shell, fibre, frond, palm kernel cake waste and EFB. Palm oil mills generate 14% fibre, 7% shells and 23% EFBs per ton of fresh fruit bunches (Omar et al. 2011). The utilisation of these byproducts has attracted much interest. The EFB and fronds are further processed into paper and paperboard, while fibres and shells can be utilised as boiler fuel to generate steam in palm oil mills (Harsono et al. 2016).

The EFB is a lignocellulosic residue and potential raw material for pulp fibre due to the availability in large quantity, continuous supply and low lignin and high cellulose contents. In particular, EFB is promising for the use as paper packaging material because Malaysia produces many vegetables, which need to be transported utilising packaging material. Gas, moisture and water resistance are required to use EFB paper as packaging material. With respect to

byproducts, it is better to use fine fibre, including EFB nanofibre, which contributes towards increased gas and water resistance properties (Lavoine et al. 2012). Furthermore, it is easier to fibrillate chemical EFB pulp fibre by beating than chemical wood pulp fibre, indicating that the structure of the EFB pulp fibre is flexible and easy to miniaturise (Kose et al. 2014). This benefits the low-energy production of fine fibre including nanofibre.

In this study, EFB pulp fibre was prepared using soda-anthraquinone pulping and bleaching. The study investigated the miniaturising behavior of EFB pulp fibre using ACC (Kondo et al. 2014). The ACC can produce various bionanofibres from natural fibre material such as cellulose, chitin and collagen by using only water (Kose et al. 2011, Kose & Kondo 2011, Kondo et al. 2014). Furthermore, the sheet prepared from fine fibre produced by ACC, was used to investigate the wettability. Various EFB pulping processes have been studied (Aziz et al. 2002, Rushdan et al. 2007, Tanaka et al. 2004). Compared with kraft cooking, soda-anthraquinone cooking is a

sulfur-free cooking process, which is preferable and more suitable to cook non-woody materials, considering environmental aspects (Harsono et al. 2016). Therefore, soda-anthraquinone pulping was used in this study to cook EFB.

MATERIALS AND METHODS

Material

The EFB employed in this study was obtained from Malaysia and had been washed, dried and defibrated to prepare the EFB fibres. Commercial bleached hardwood kraft pulp (hardwood pulp) was used as reference material.

Pulping of EFB fibre

The EFB fibre was cut to a length of 2 to 3 cm. The EFB fibres were cooked using the soda-anthraquinone process. The cooking liquor consisted of 16% active alkali (Na_2O equivalent) with 0.05% anthraquinone. The cooking temperature was 170 °C with a duration of 2 hours. It took one hour to reach the cooking temperature from room temperature. The ratio of the EFB fibre content to the liquid (liquid ratio) was 9%. The EFB fibres were washed with a sufficient amount of water after cooking and separated on a flat screen to obtain the EFB pulp fibre. The EFB pulp fibres were bleached with acetic acid and sodium chlorite.

Aqueous counter collision treatment

The ACC treatment was conducted using Star Burst Labo. The pulp fibre suspension was poured into the equipment for the treatment. The number of collision and ejecting pressure were set to 0 to 50 passes and 200 MPa, respectively. Each treated suspension, at 0.03–0.05% fibre concentration, was poured into a vial and kept for a day under similar fibre concentration. The height of the precipitation, including fibre, was measured to investigate the miniaturisation behavior of the pulp fibre. Fibre after ACC treatment is referred to as fine fibre.

Characterisation of original pulps

The pulp fibre length was measured according to ISO 16065-2 and the length-weighted mean fibre length was determined. To measure the

zero-span tensile index of the fibre, handsheets were prepared according to ISO 5269-1. The zero-span tensile index was measured according to ISO 15361.

Observation of the fibre

The fine fibre was analysed using an optical microscope with field lens (numerical aperture: 0.10) and a scanning electron microscope. The freeze-dried sample was used for SEM observations. Before freezing the sample, the water of the fibre suspension was first replaced to ethanol and then to t-butyl alcohol. Subsequently, the suspension was rapidly frozen using liquid N_2 and freeze-dried. The freeze-dried sample was spattered with Pt. The acceleration voltage was set to 2 kV during the observation. The acquired images were used for measurements of the width of individual fibres. The total number of measurements was 50 for each fibre sample.

Preparation of the fine fibre sheet

To prepare the sheets using these fibres, the concentration of the suspension was adjusted to 0.2%. The suspension was filtered through a membrane filter (material: mixed cellulose ester) with a pore size of 0.45 μm under reduced pressure, resulting in a wet sheet including almost all fibres. This wet sheet and the membrane filter were placed on a paper towel that acted as water-absorption material on top of the membrane filter, and Teflon sheet was placed on the wet sheet. The assembled sheet was held by the heated metal plates of a hot press at a temperature of 105 °C and pressure of 90 kPa for 10 min to obtain a dried sheet composed of fine fibres.

Wettability measurement

Figure 1 shows the schematic view of the equipment used to measure the wettability of the sheets (Yoshinaga et al. 1993, Okayama et al. 2004). The equipment consists of a single-lens reflex camera, bellows attachment, wide-angle lens, stage, syringe and light. The sheet was attached to the slide glass using double-sided tape. The contact surface between the sheet and the double-sided tape was the side of the sheet, touching the Teflon sheet during drying. Images were obtained every 0.2 s, for

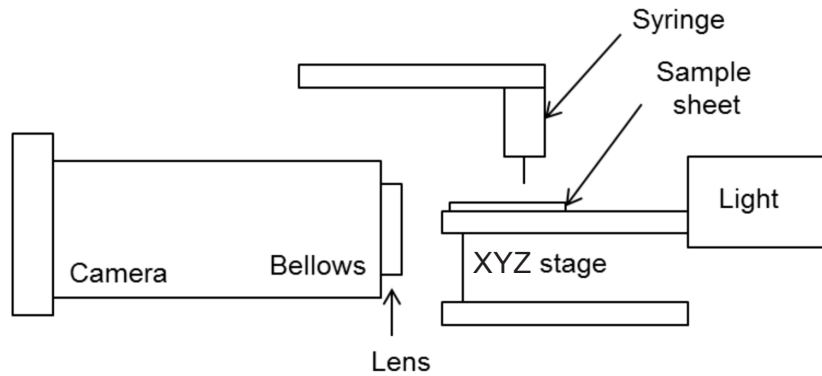


Figure 1 Schematic view of the equipment used to investigate the wettability of the sheets

10 s, using the camera, with a drop of ion exchange water that was passed using a syringe (0.22- μm membrane filter) to the sheet at 23 °C and 50% RH. The obtained images were analysed using Image-Pro Premier 9.1 where the contact angle, volume of water on the sheet and diameter of the interface between the water and sheet were measured. The image capture and measurement were repeated three times.

RESULTS AND DISCUSSION

Properties of the EFB pulp

The length-weighted mean length of the EFB pulp fibre and the hardwood pulp fibre were 0.66 mm and 0.68 mm, respectively. Figure 2 shows the distribution of length-weighted mean length of both pulp fibres. The difference between the length-weighted mean lengths of both pulp fibres is small, showing that the distribution of EFB pulp fibre is different from hardwood; shorter fibres with less than 0.2 mm in EFB pulp fibre is more than those of the hardwood. Furthermore, the EFB pulp fibre with a width of 20.6 ± 9.5 μm was almost same as the hardwood pulp fibre (19.4 ± 6.2 μm of width).

The zero-span tensile indices of the EFB and hardwood pulp fibre handsheet are 6.0 ± 0.3 kN.mg^{-1} and 9.2 ± 0.6 kN.mg^{-1} , respectively. The zero-span tensile index has often been used as an index of the single-fibre strength (Page 1969). Notably, the fibre strength of the EFB pulp fibre is lower than that of hardwood pulp fibre, indicating that the single-fibre strength of the EFB pulp fibre is also lower.

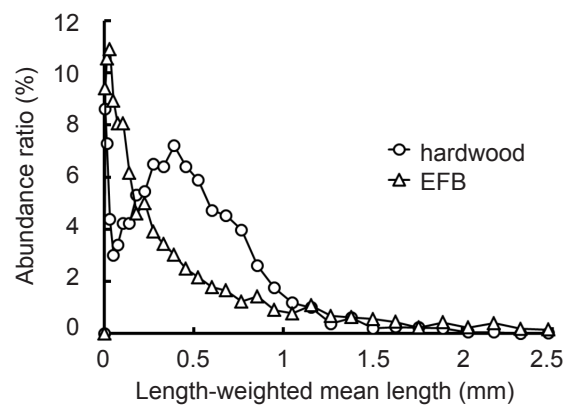


Figure 2 Distribution of length-weighted mean length of the EFB pulp fibres and hardwood pulp fibres

Behavior of the EFB pulp fibre during ACC treatment

Figure 3 shows the change of the precipitation volume with increasing number of collision under same the concentration of fibre. Notably, both EFB and hardwood pulp fibre precipitation volumes increased from 0 to 10 collisions. The volume tends to increase with progressing miniaturisation of the pulp fibre (Saito et al. 2006, Tsuboi et al. 2014). Therefore, the miniaturisation of both pulp fibre types progresses until at least 10 collisions. Figure 4 shows the miniaturisation behavior of the EFB and hardwood pulp fibre with increasing number of collision. The resolution of the optical microscopy is almost 3 μm . Therefore, it is difficult that the fibre with less than 3 μm of width is observed using the optical microscope. The EFB fibres could not be observed after 10 collisions by optical microscopy, while hardwood fibres were observed. The fibres produced

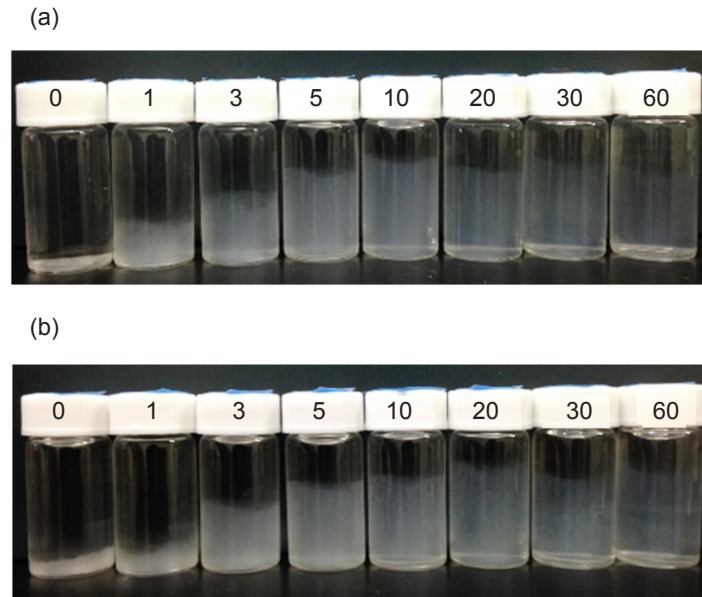


Figure 3 Change of the precipitation volume with increasing number of collision, a = EFB pulp fibre sample, b = hardwood pulp fibre sample; the numbers in a and b indicate the number of collision

from hardwood pulp fibre disappeared after 20 collisions. It is easier to miniaturise the EFB pulp fibre at 200 MPa compared with hardwood pulp fibre in the range of more than 3 μm of fibre size.

Figure 5 shows the SEM images of the EFB and hardwood pulp fibre samples after 60 collisions. These samples could not be observed by optical microscopy (Figure 4). However, many fibres could be observed on the nanoscale using SEM. The widths of the EFB and hardwood pulp fibre samples were 14 ± 3 nm and 16 ± 4 nm, respectively. The coating thickness was approximately 5 nm in a condition of the SEM observation. It was possible that the lateral dimension of the fibres was unchanged by the coating, since the Pt was sputtered onto the sample (Abe et al. 2007).

Wettability of the fine fibre sheet

The sheets were formed using fine fibres, prepared from EFB and hardwood pulp fibre by ACC treatment, in order to investigate the wettability of the fine fibre sheet. The density of the fibre sheet would be an important factor influencing wettability, because water droplets can penetrate the pores of pulp fibre handsheet. The rate of water penetration into the fine fibre sheet would be slower than pulp fibre handsheet, because the pore volume of fine fibre sheet was significantly lower. In Figure 6, the densities of

the sheets are shown as a function of the number of collisions. The densities of the fine fibre sheets increased with an increase in the number of collisions. The fine fibre sheet densities for EFB pulp fibre were similar to hardwood pulp fibre under the same number of collisions, during ACC treatment. As shown in Figure 4, small fine fibres, less than 3 μm in width included in EFB samples, were higher in number than hardwood sample, therefore the density of the EFB fine fibre sheet was higher than hardwood fine fibre sheet. However, the densities of both samples were almost the same under similar number of collisions. Further investigation is required to clarify the relationship between the density of the sheet and the size of the fine fibres.

Figure 7 shows the volume change of water drops on fine EFB and hardwood fibre sheets, for the determination of whether the water drop penetrated each sheet within 10 s. In the case of both the pulp fibre sheets not subjected to ACC treatment, the drop was quickly absorbed by the sheet within 1 s after it contacted the sheet surface, and therefore it was not easy to measure the drop volume on the fibre sheet. The volume of water drops on the fine fibre sheets, except for sheet subjected to 3 collisions for the EFB pulp fibre, barely decreased during the 10 s, indicating that the drop did not penetrate both fine fibre sheets within 10 s. After ACC treatment, the density of the sheet could not influence water

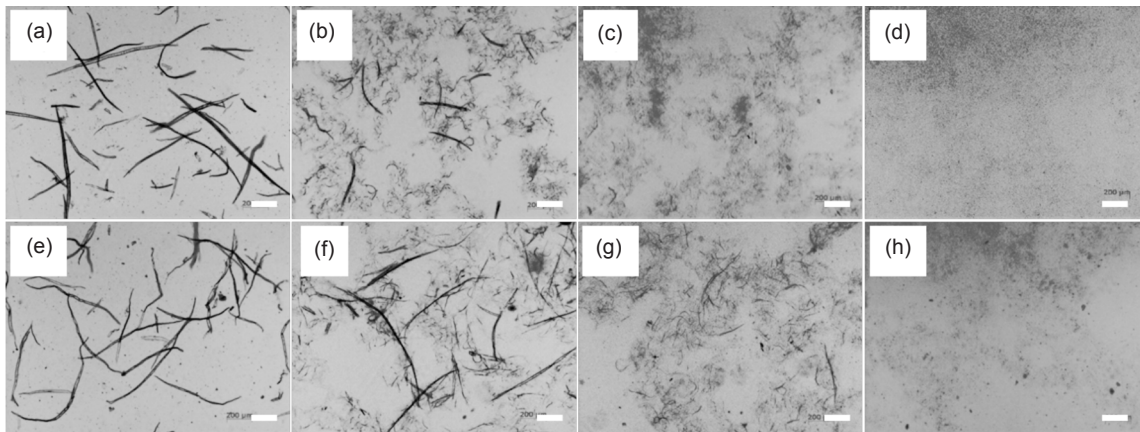


Figure 4 Optical microscopy images of the EFB and hardwood pulp fibre samples before and after ACC treatment; EFB sample: a = before ACC treatment, b = 3 collisions, c = 10 collisions, d = 60 collisions; hardwood pulp fibre sample: e = before ACC treatment, f = 3 collisions, g = 10 collisions, h = 60 collisions; bars = 200 µm

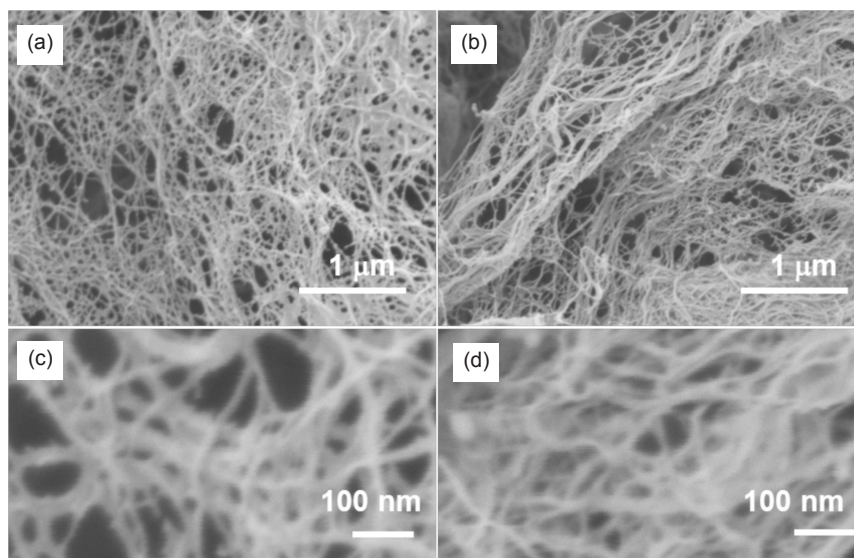


Figure 5 Scanning electron microscopic (SEM) images: a & c = fine fibres of EFB, b & d = hardwood fine fibre, prepared by ACC at 200 MPa and 60 collisions

penetration within 10 s. One possible explanation for the suppression of water penetration into ACC-treated sheet was the high surface density of the sheet. The finer fibres were produced during ACC treatment, deposited on the surface of the membrane filter under vacuum filtration. Therefore, the surface of the sheet contacting the membrane filter had many finer fibres, resulting in a high surface density of the sheet. Once the high density surface was produced, the drop of water could not penetrate the sheet, irrespective of the bulk density of the sheet.

To study the wettability of the EFB fine fibre sheet, and compare it with hardwood fine fibre

sheet, images were obtained for the contact line and profile history of a water drop on the surface of the fine fibre sheet at 1 s intervals. Changes in contact angle and diameter of contact line of the water drop were determined from a series of photographs of the drop silhouette by referring to previous reports (Okayama et al. 1985, Okayama et al. 1987). As shown in Figure 8, the water contact angle on ACC-treated sheets, prepared from EFB pulp fibre, decreased gradually during the initial 5 s after water contacting the sheet surface. After 5 s, the contact angle caused a significant delay in the decrease of the contact angle with time.

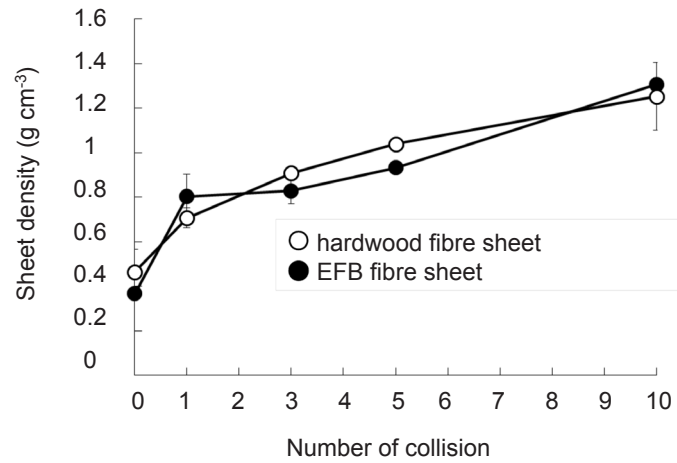


Figure 6 Change of the fine fibre sheet density prepared from EFB pulp fibre and hardwood pulp fibre with increasing number of collision

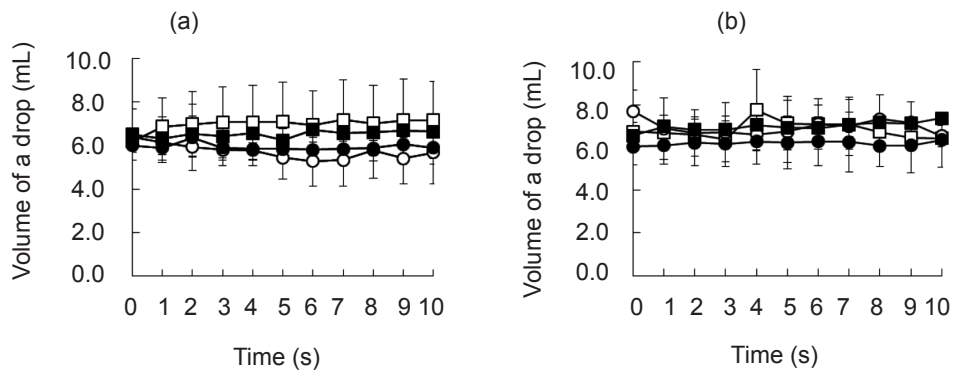


Figure 7 Change of volume of a drop on a fine fibre sheet over time after drop contact, a = EFB, b = hardwood, □ = 1 collision, ○ = 3 collisions, ■ = 5 collisions, ● = 10 collisions

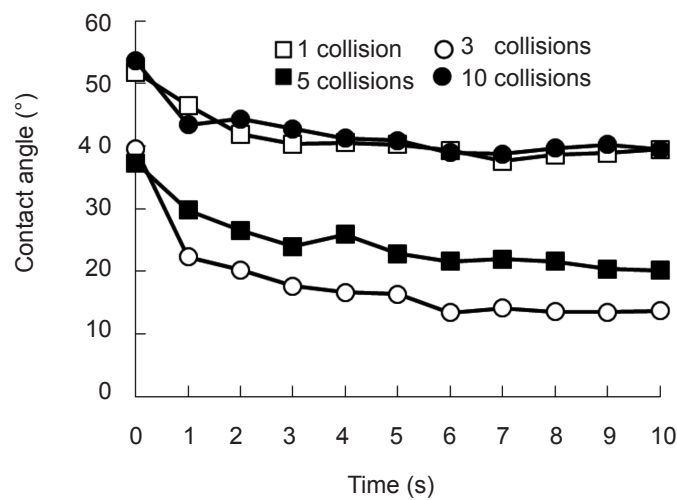


Figure 8 Change of the contact angle of fine fibre sheet prepared from EFB pulp fibre with time after water contact; graph legends shows number of collision

Therefore, the study focused on the contact angle at 6 s, as shown in Figure 9. The contact angle of the fine EFB fibre sheet first decreased from 1 to 3 collisions and then increased up to 10 collisions. The contact angle of fine hardwood fibre sheet also gradually decreased from 1 to 5 collisions, and then increased. Notably, the change in the contact angle of the fine EFB fibre sheet was larger than hardwood sheet, in the range of 1 to 10 collisions. Figure 10 shows the change in the diameter of the drop on the sheet over time, after the drop contacted the sheet. The diameter of the drop on all sheets increased notably within the initial 2 s. The diameter of the water drop on the fine EFB and hardwood sheet, treated with 3 and 5 collisions was larger than that of the sheet treated with 1 and 10 collisions. This trend corresponds to that noted for contact angle (Figure 9). Normally, a contact angle is

low when the diameter of a water drop is large on a sheet without water penetration into the sheet. According to Figures 7–10, the decrease in contact angle, as shown in Figure 8, could be mainly attributed to the spread of the drop on the surface. Further investigations are needed to understand the reason why the contact angle of fine EFB fibre sheet first decreased, and then increased from view point of surface roughness and surface free energy of the sheet.

CONCLUSIONS

In this report, the miniaturisation behavior of EFB pulp fibre and the wettability of fine EFB fibre sheet, compared to hardwood pulp fibre and its fine fibre sheet, were investigated. It was easier to miniaturise EFB pulp fibre with low single-fibre strength compared with hardwood

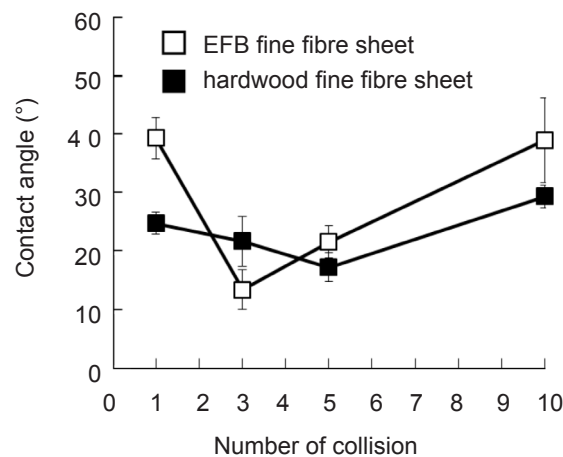


Figure 9 Change of contact angle of fine fibre sheet, prepared from EFB and hardwood pulp fibre with increasing in number of collision after 6s following drop contact

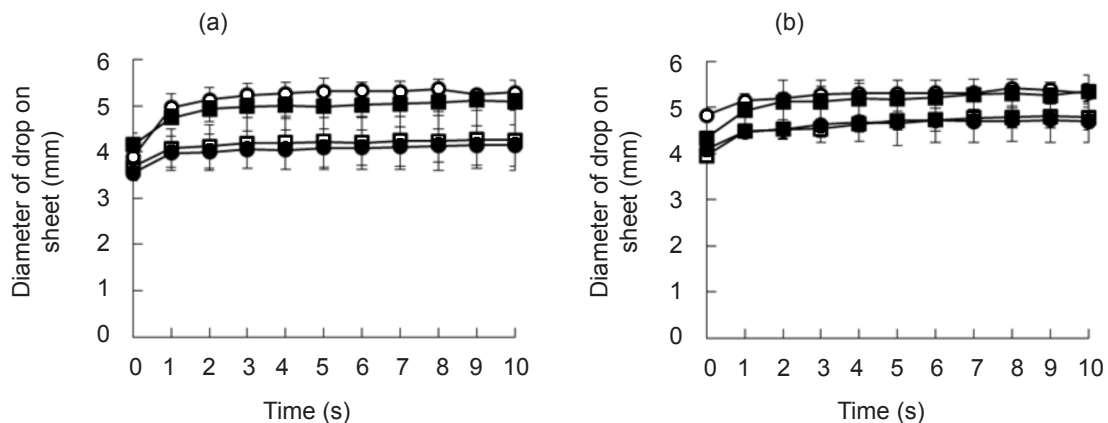


Figure 10 Change of drop diameter on the sheet over time after drop contact, a = EFB, b = hardwood, □ = 1 collision, ○ = 3 collisions, ■ = 5 collisions, ◆ = 10 collisions

pulp fibre, during ACC treatment. Fine fibres with a width of less than 15 nm were prepared from EFB pulp fibre after ACC treatment sufficiently. The width of fine fibre was almost the same as hardwood pulp fibre. The dependence of wettability of fine EFB fibre sheet on the number of collisions was similar to that observed for fine hardwood fibre sheet. Interestingly, the water contact angles of both fine fibre sheets at 6 s, after the initial contact, first decreased and then showed a tendency to increase up to 10 collisions.

REFERENCES

- ABE K, IWAMOTO S & YANO H. 2007. Obtaining cellulose nanofibres with a uniform width of 15 nm from wood. *Biomacromolecules* 8: 3276–3278.
- AZIZ AA, HUSIN M & MOKHTAR A. 2002. Preparation of cellulose from oil palm empty bunches via ethanol digestion: effect of acid and alkali catalysts. *Journal of Oil Palm Research* 14: 9–14.
- FAO. 2014. Crops/Malaysia/Production Quantity/Oil, Palm fruit/2014. <http://faostat3.fao.org/>
- HARSONO H, PUTRA AS, MARYANA R ET AL. 2016. Preparation of dissolving pulp from oil palm empty fruit bunch by prehydrolysis soda-anthraquinone cooking method. *Journal of Wood Science* 62: 65–73.
- KONDO T, KOSE R, NAITO H & WAKAKO K. 2014. Aqueous counter collision using paired water jets as a novel means of preparing bio-nanofibres. *Carbohydrate Polymers* 112: 284–290.
- KONDO T, KUMON D, MIENO A, TSUJITA Y & KOSE R. 2014. Preparation and characterization of two types of separate collagen nanofibres with different widths using aqueous counter collision as a gentle top-down process. *Materials Research Express* 1: doi 10.1088/2053-1591/1/4/045016
- KOSE R, KIMURA T, AZIZ MKA & OKAYAMA T. 2014. Recycling effects on the properties of pulp fibre sheets produced from oil palm empty fruit bunch. *Sen-I Gakkaishi* 70: 259–264.
- KOSE R & KONDO T. 2011. Favorable 3D-network formation of chitin nanofibres dispersed in water prepared using aqueous counter collision. *Sen-I Gakkaishi* 67: 91–95.
- KOSE R, MITANI I, KASAI W & KONDO T. 2011. “Nanocellulose” as a single nanofibre prepared from pellicle secreted by *Gluconacetobacter xylinus* using aqueous counter collision. *Biomacromolecules* 12: 716–20.
- LAVOINE N, DESLOGES I, DUFRESNE A & BRAS J. 2012. Microfibrillated cellulose - its barrier properties and applications in cellulosic materials: a review. *Carbohydr Polym* 90: 735–64.
- OKAYAMA T, KIMURA S & OYE R. 1985. Measurement on dynamic wettability of paper surface. *Japan TAPPI Journal* 39: 1157–1163.
- OKAYAMA T, OCHI T & OYE T. 1987. Measurement on dynamic wettability of paper surface. Part 2. *Japan TAPPI Journal* 41: 515–522.
- OKAYAMA T, YOSHINAGA N & HASHIZUME K. 2004. Liquid transfer characteristics of recycled pulp handsheets. *Japan TAPPI Journal* 58: 92–100.
- OMAR R, IDRIS A, YUNUS R, KHALID K & AIDA ISMA MI. 2011. Characterization of empty fruit bunch for microwave-assisted pyrolysis. *Fuel* 90: 1536–1544.
- PAGE DH. 1969. A theory for the tensile strength of paper. *Tappi* 52: 674–681.
- RUSHDAN I, LATIFAH J, HOI WK & MOHD NOR MY. 2007. Commercial-scale production of soda pulp and medium paper from oil palm empty fruit bunches. *Journal of Tropical Forest Science* 19: 121–126.
- SAITO T, NISHIYAMA Y, PUTAUX JL, VIGNON M & ISOGAI A. 2006. Homogeneous suspensions of individualized microfibrils from TEMPO-catalyzed oxidation of native cellulose. *Biomacromolecules* 7: 1687–1691.
- TANAKA R, WAN RWD, MAGARA K, IKEDA T & HOSOYA S. 2004. Chlorine-free bleaching of kraft pulp from oil palm empty fruit bunches. *Jarq-Japan Agricultural Research Quarterly* 38: 275–279.
- TSUBOI K, YOKOTA S & KONDO T. 2014. Difference between bamboo- and wood-derived cellulose nanofibres prepared by the aqueous counter collision method. *Nordic Pulp and Paper Research Journal* 29: 69–76.
- YOSHINAGA N, OKAYAMA T & OYE R. 1993. Measurement of wettability of pulp fibre at short time intervals. *Sen-I Gakkaishi* 49: 287–293.